International Journal of ChemTech Research
CODEN (USA): IJCRGG, ISSN: 0974-4290, ISSN(Online):2455-9555
Vol.10 No.10, pp 361-376, 2017

Experimental and theoretical study of D-Biotin as green Inhibitors on the corrosion inhibition of carbon steel in Chloride ion environment

Albin Aloysius[1]*, Rajajeyaganthan Ramanathan[2], Auxilia Christy[1], Noreen Anthony[3]*

[1]Department of Chemistry, BWDA Arts & Science College, Kolliyangunam – 604304, Tamilnadu, India
[2]Department of Chemistry, Kalasalingam Academy of Research and Education, Kalasalingam University, Krishnankoil 626126, Tamil Nadu, India
[3]Department of Chemistry, Holy Cross College, Tiruchirappalli – 620002, Tamilnadu, India

Abstract : Electrochemical impedance, Potentiodynamic polarization and weight loss studies were performed on carbon steel in 240ppm Chloride ion solution with various concentrations of D-Biotin as inhibitors, The results of potentiodynamic polarization showed that i_{corr} (corrosion current density) decreases with increasing the concentration of biotin showing a decrease in the corrosion rate as well as an increase in the inhibition efficiency of carbon steel. The observed results show that biotin is good corrosion inhibitors. Surface analysis using UV-Vis, FTIR, SEM, EDX spectra, Adsorption isotherm and Thermodynamic parameter of these inhibitors in 240 ppm Chloride ion medium shows that biotin act as good corrosion inhibitors. Quantum chemical data obtained from DFT (density functional theory) calculations agree with this experimental results.
Keywords: Potentiodynamic, polarization, Electrochemical impedance spectroscopy, Biotin, Carbon steel, Chloride ion medium.

1. Introduction

The process of cooling water circulation systems is met with numerous challenges; among this, the most important is corrosion of the metal equipment. Substances dissolved in cooling water may have unlike effects on the corrosion of metals. The corrosion of iron in corrosive environments, particularly in cooling water having chloride, reduces its uses. The mechanisms of pitting and crevice corrosion are comparable and they most frequently occur in chloride environments.[1-3] Chloride and sulfate ions harmfully affect the most metals and the presence of 100 ppm chloride ions in the water causes pitting corrosion of steel.[4]Natural products and drugs in different atmosphere for several metals act as corrosion inhibitors.[5-7]Study on organic compounds having hetero atoms such as S, P, N, O and compounds having multiple bonds inhibit corrosion of metal by surface adsorption.[8-17] cooling water systems contain several types of corrosion and their inhibitor are studied in detail.[18] green inhibitors like vitamins[19] on corrosion of metals and their inhibition efficiency on corrosion of metals in chloride[20] and acid[21-26] medium were studied in detail. In vitamins, B vitamins are water-soluble chemically distinct vitamins but their use as corrosion inhibitors are not studied well in Chloride ion environment.

Among the water soluble B vitamins family Biotin (vitamin B7) is the one which is required in our health system. The structure of biotin is given in Figure 1. It consists of two rings, an ureido and a thiophene ring but fused together through one of its sides. Biotin is naturally present in peanuts and leafy green vegetables. In this research, weight loss method, UV-Vis, FT-IR, potentiodynamic polarization curves and electrochemical impedance, spectroscopy were used to study the corrosion inhibition effect of biotin on corrosion of carbon steel in 240 ppm Chloride ion solution.

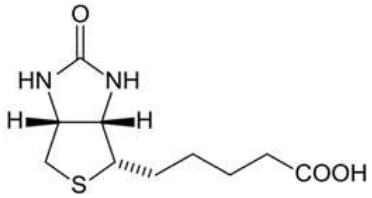

Figure 1. Structure of biotin

2. Experimental

2.1. Material and coupons

The carbon steel was used as a test material with a chemical composition of 0.10% C, 0.06% P, 0.40% Mn, 0.026% S, and the balance of Fe. Coupons with 1 x 4 x 0.2 cm^3size were cut and abraded their surfaces using 150–600 grit emery sheets, and then the coupons were degreased with acetone and washed with de-ionized water before testing. $FeSO_4$ and Chloride ion were purchased from Merck, India. Biotin was purchased from Loba Chemie, India. In the preparation of biotin solution,1g Biotin is dissolved in 2ml of 13M ammonia and made up to 100 ml in a SMF using double distilled water. Chloride ions concentration of 240 ppm and various concentrations of ferrous ions were prepared using double distilled water. Corrosion medium is a fixed concentration of 240 ppm of chloride ions in double distilled water. Inhibitors concentration of 25, 50, 100, 150 and 200 ppm were used to find out corrosion rate and inhibition efficiency.

2.2. Weight loss method

In this method, every single test was carried out in a vessel of glass having 100 mL of 240 ppm Chloride ion solution. All the experiments were carried out at a room temperature of 30° C by dipping the carbon steel coupons using glass hooks in 100 mL of the blank solutions or solution with inhibitor. After 24 h immersion, the coupons were taken out from solution, rinsed with double distilled water, dried thoroughly and weighed.

The weight loss was used to calculate the corrosion rate denoted as CR, ($mg.dm^{-2}day^{-1}$) and the inhibition efficiency as IE, (%):

$$CR\ (mg.dm^{-2}.day^{-1}) = W = \frac{M1-M2}{SP}$$

Where, M_1 and M_2 is the mass of the coupons before and after the corrosion respectively, S is the surface area of the coupons in dm^2, P is the period of immersion in days, and W is the corrosion rate. The IE was calculated by using the following equation:

$$IE\ (\%) = \frac{(W_0-W_i)}{W_0} \times 100$$

Here $\Delta W = (W_0 - W_i)$, where W_0 and W_i are the corrosion rate of carbon steel in the absence and presence of inhibitor respectively,

In this study, the CR value is calculated using the formula,

$$CR\ (mg.dm^{-2}.day^{-1}) = M_1\text{-}M_2\ (mg)/\ [0.096\ (dm^2) \times 1\ day]$$

where, the surface area S takes the value of 0.096 dm^2.

2.3. Potentiodynamic polarization studies

Electrochemical experiments were carried out using conventional three electrode cell assembly. The working electrode was a carbon steel coupon with an exposed surface area of 1 cm^2 was fitted to a holder and the rest of the area was covered with epoxy coating. Saturated calomel electrode and platinum wire were used as reference and counter electrode. The working electrode was vertically immersed in the test solution and open circuit potential was recorded by using Princeton Applied Research (2 channels) analyzer. With respect to open circuit potential value, the Tafel polarization studies were carried out at a scan rate of 0.5 mV/s. Corrosion current (I_{corr}) and corrosion potential (E_{corr}) were obtained by extrapolating the anodic and cathodic curves of Tafel plot. Inhibition efficiency was calculated by using respective I_{corr} values. Electrochemical impedance analyses were performed in the frequency range from 1 Hz to 1MHZ with amplitude of 10 mV peak-to-peak using AC signal at E_{corr}. The carbon steel coupons used for this study have a surface area of 1 cm^2,which were exposed to the corrosive solution. All these measurements were done at the atmospheric conditions without any stirring. The experiments were conducted in the absence and presence of inhibitor with different concentration in the 240 ppm Chloride ion medium.

2.4. Characterization of surface morphology

Surface morphologies of the films were mainly observed under scanning electron microscopy, SEM (TESCAN Vega 3) using electron acceleration between 5 and 10 kV.

2.5. Fourier transforms infrared (FT-IR) spectroscopy

FT-IR spectra were recorded in Perkin Elmer Spectrum RX I with a spectral range of 4000 cm^{-1} to 400 cm^{-1} and a spectral resolution of 4 cm^{-1}. The carbon steel coupons were immersed for 24 h in 100 mL of 240 ppm of Chloride ion medium containing various concentrations of vitamins. After 24 h, the coupons were taken out and dried. Finally, the coupons were rubbed with a small amount of KBr powder and made into a disk for FTIR characterization.

2.6. UV-Visible spectroscopy

The UV-Visible absorption spectra of 240 ppm Chloride ion solution containing various concentrations of Biotin and the same solution with 300 ppm of ferrous ion were recorded using PerkinElmer's Lambda 35 UV-Vis spectrophotometer with a spectral range of 190 nm to 1100 nm.

2.7. Computational methods

All calculations were done by using the Gaussian 03 software. The molecular structure optimization was done by quantum chemical calculations performed using density function theory (DFT)/B3LYP method (Becke's three parameter hybrid Hartree-Fock and Lee-Yang-Par correlation functional theory) with basis set 6-31G*. Energy of highest occupied molecular orbital (HOMO) and lowest unoccupied molecular orbital (LUMO), the energy gap between E_{LUMO} and E_{HOMO} ($\Delta E = E_{LUMO} - E_{HOMO}$), dipole moment ($\mu$), and other parameters were obtained from the theoretical studies forD-Biotin.

3. Result and discussion

3.1. Weight Loss Measurement

The values of corrosion behavior of carbon steel in 240 ppm Chloride ion solution in the absence and presence of various concentration of inhibitor from weight loss measurements are given in Table 1 and figures 2(a) and 2(b). From this study, the IE (%) increases with increase in concentration of the inhibitor. The maximum efficiency 91.37% is obtained at 200 ppm of D-Biotin solution after 24 h of immersion time of carbon steel specimens. In figure 2(a), the IE (%) is increasing with inhibitor concentration and the maximum efficiency is reached at a concentration of 200 ppm. On further increasing the inhibitor concentration (250 and 300 ppm) does not show any appreciable change in the efficiency. The reason for this study may be that all the active sites of surface of carbon steel are completely adsorbed by the inhibitor molecule and there is no empty active sites are available for further adsorption.

Figure 2(b) shows that the CR of carbon steel decreases from 16.56 $mgdm^{-2}day^{-1}$to 3.39$mgdm^{-2}day^{-1}$ on the addition of 25 ppm to 200 ppm of inhibitor after 24 h of immersion time. The increase in IE (%) from 57.87% to 91.37% may be due to the blocking effect of the metal surface by adsorption and film formation mechanisms, which decreases the effective area of corrosion attack [19]. From the weight loss measurements, the inhibiting performance exhibited by the compound may be due to the presence of donor oxygen atom and π electron of benzene ring, which makes it adsorb and form insoluble protective layer on the surface of mild steel. From these results, it is clear that the studied inhibitor D-Biotin is quickly adsorbed at the corrosion active sites of carbon steel surface and responsible for anticorrosion activity.

Table 1.Percentage inhibition efficiencies and corrosion rates values obtained from the weight loss of mild steel in 240 ppm chloride ion in the absence and presence of various concentrations of inhibitors

Conc. of PABA (ppm)	30°C		40°C		50°C		60°C	
	CR (mg.dm-2.day-1)	IE (%)	CR (mg.dm-2.day-1)	IE (%)	CR (mg.dm-2.day-1)	IE (%)	CR (mg.dm-2.day-1)	IE (%)
Blank	39.33	-	39.33	-	39.33	-	39.33	-
25	16.56	57.87	24.20	38.46	27.01	31.32	30.17	23.27
50	14.19	63.90	27.01	58.62	30.17	47.48	14.19	35.48
100	11.17	71.59	30.17	68.96	14.19	57.08	16.27	41.12
150	6.783	82.75	14.19	74.92	16.27	61.02	20.65	44.02
200	3.391	91.37	16.27	77.91	20.65	62.54	25.37	45.43

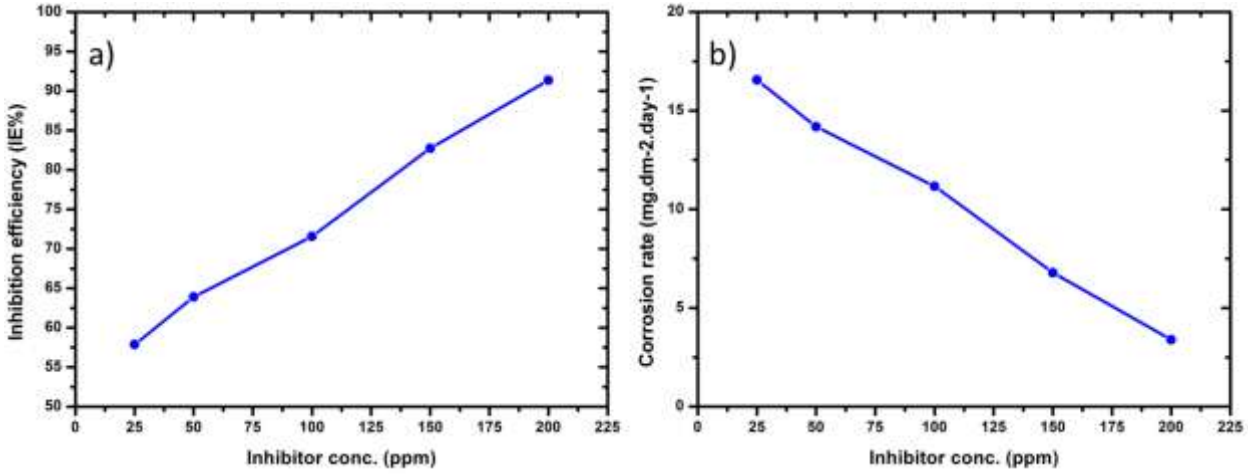

Figure 2. Weight loss curves of various concentrations of inhibitor in 240 ppm Chloride ionsolution at room temperature: (a) variation of IE (%) with different concentrations of inhibitor and (b) variation of CR with different concentrations of inhibitor.

3.2.pH Study

Corrosion rates of carbon steel in 240 ppm aqueous chloride ion environment in optimum inhibitor concentration (200 ppm) decreases with increase in the pHup to pH 7 then it started increasing similarly Inhibition efficiency increases with increase in the pH up to pH 7 then it started decreasing it shows that at neutral pH adsorption of inhibitor on the metal surface is maximum.

Table 2. Weight loss studies of carbon steelin various pH in 240 ppm Chloride ion solution.

pH	Weight loss (mg.dm-2)	CR (mg.dm-2.day-1)	Surface coverage (θ)	IE (%)
Blank	3.93	39.33	-	-
3	3.36	33.62	0.1450	14.50
5	1.91	19.11	0.5140	51.40
7	0.33	3.39	0.9137	91.37
9	1.23	12.30	0.6870	68.70
11	3.13	31.38	0.2020	20.20

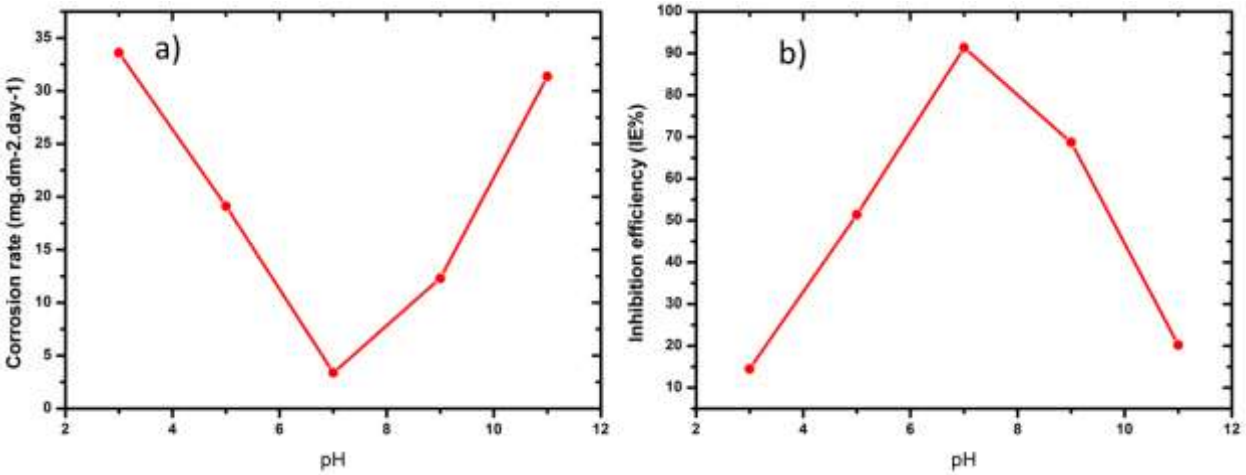

Figure 3. Weight loss curves of optimum concentrations of inhibitor in 240 ppm Chloride ion solution at different pH: (a) variation of CR with different pH and (b) variation of IE (%) with different pH

3.3 Adsorption isotherm

Adsorption isotherms are very important in understanding the mechanism of inhibition of corrosion reactions of metals and alloys. The most frequently used adsorption isotherms are the Frumkin, Temkin and Langmuir isotherms. Attempts to fit data obtained from the weight loss measurements into different adsorption isotherms reveal that the data best fitted the Langmuir adsorption isotherm. For further discussion instead of Biotin (vitamin B7), VB7 was used to make it simple. Assumptions of Langmuir relate the concentration of the adsorbate in the bulk of the electrolyte (C_{inh}) to the degree of surface coverage (θ) as Equation given below:

$$\frac{C_{inh}}{\theta} = \frac{1}{K_{ads}} + C_{inh}$$

Table 3. Thermodynamic adsorption parameters for carbon steel in 240 ppm of Chloride ion in the presence of optimum concentrations of VB7 at different temperatures

Temperature (K)	R^2	K_{ads} (10^3/ppm)	ΔG_{ads} (kJmol-1)
303	0.9845	36.64	-177.04
313	0.9998	29.61	-165.25
323	0.9984	25.13	-138.42
333	0.9985	19.34	-35.33

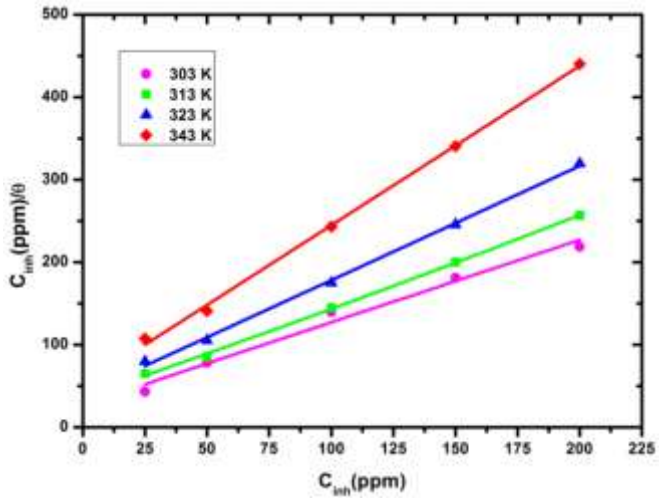

Figure 4. Langmuir adsorption isotherm plots for the adsorption of VB7 in 240 ppm Chloride ion on the surface of mild steel

where K_{ads} is the equilibrium constant of adsorption. The linear regressions parameters between C_{inh}/θ and C_{inh} are listed in Table 3. Figure 4 shows the straight lines of C_{inh}/θ versus C_{inh} at different temperatures. These results show that all the linear regression coefficients (R) are close to 1, which confirms that the adsorption of VB7 on the steel surface obeys the Langmuir adsorption isotherm. The slope of the C_{inh}/θ versus C_{inh} plots show a deviation from unity, which means nonideal simulating [27] and is unexpected from the Langmuir adsorption isotherm. It might be the result from the interactions between the adsorbed species on the carbon steelsurface [28-29]. The adsorption equilibrium constant (K_{ads}) and free energy of adsorption(ΔG^{o}_{ads}) were calculated using the following relationship:

$$\Delta G^{o}_{ads} = -RT \ln (55.5\ K_{ads})$$

where 55.5 is the concentration of water in solution in mol L^{-1} and R is the universal gas constant. Table 3 reveals that the K_{ads} decreases with increasing temperature, which indicates that it is easily and strongly adsorbed onto the steel surface for the inhibitor at a lower temperature. But when the temperature is high, the adsorbed inhibitor tends to desorb from the steel surface. Generally, values of ΔG^{o}_{ads} around -20 kJ mol^{-1} or lower are consistent with the electrostatic interaction, and when it is around -40 kJ mol^{-1} or higher, then this is a chemical interaction [30]. Here, the calculated ΔG^{o}_{ads} values are between -177.04 and -35.33 $kJmol^{-1}$, indicating that the adsorption mechanism of VB7 on carbon steelin 240 ppm Chloride ionsolution at the studied temperatures is predominantly chemisorption (molecular). The negative values of ΔG^{o}_{ads} ensure that the adsorption of inhibitor molecule onto the steel surface is a spontaneous process.

3.4 Thermodynamic parameters

Thermodynamic parameters are important to understand the inhibition mechanism. The thermodynamic functions for dissolution of carbon steel without and with addition of various concentrations of VB7 were calculated from the logarithm of the corrosion rate (CR) of metal in 240 ppm Chloride ion solution by using the Arrhenius equation:

$$\log CR = -\frac{E_a^o}{2.303RT} + A$$

where CR is the corrosion rate, E_a^o is the apparent activation energy, A is the pre-exponential factor. Arrhenius plots of log CR versus 1/T for the blank and different concentrations of VB7 give a straight line and slope equal to $-\frac{\Delta E_a^o}{2.303R}$ shown in Fig. 5, from which the values of E_a^o for the inhibited corrosion reaction of carbon steel have been calculated and are recorded in Table 4. The values of E_a^oin the presence of optimum concentrations of VB7 are higher (917.91 kJ mol-1) than those in the blank solutions (597.88 kJ mol-1), indicating that the energy barrier of the corrosion reaction increased in the presence of the inhibitor [31].

From the transition state equation: $CR = \frac{RT}{Nh}\exp(\frac{\Delta S_a^o}{R})\exp(-\frac{\Delta H_a^o}{RT})$

where ΔH_a^o is the enthalpy of activation, ΔS_a^o is the entropy of activation, h is the Planck's constant, N is the Avogadro number, and R is the universal gas constant. The plots of log (CR/T) versus 1/T give straight lines with slope equal to $-\frac{\Delta H_a^o}{2.303R}$ and intercept ($\log\frac{R}{Nh}+\frac{\Delta S_a^o}{2.303R}$) from which ΔH_a^o and ΔS_a^o values were calculated and are listed in Table 4. The positive sign of ΔH_a^o indicates that the adsorption process is endothermic [32]. This indicates that IE % decreases with the temperature. Such behaviour can be interpreted on the basis that increasing temperature resulted in desorption of the adsorbed inhibitor molecules from the metal surface. The negative value of ΔS_a^o shows that the process of adsorption is accompanied by a decrease in entropy. The decrease in entropy suggested that in the rate determining step there is association rather than dissociation.

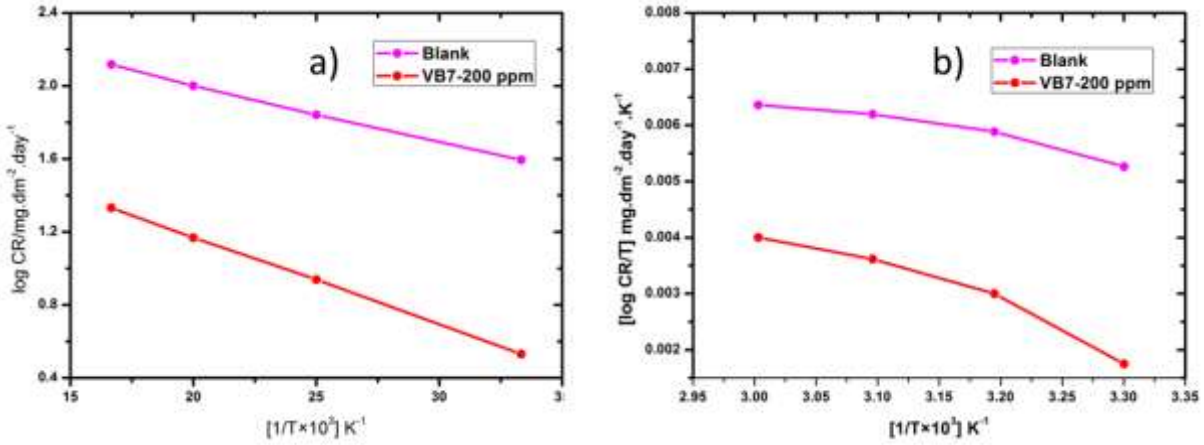

Figure 5.a)Adsorption isotherm plots for log CR versus 1/T. b) Adsorption isotherm plot for log CR/T versus 1/T

Table 4.Thermodynamic activation parameters for carbon steel in 240 ppm Chloride ion solution in the absence and presence of optimum concentrations of VB7

Inhibitors Conc (ppm)	E_a^o (kJmol-1)	ΔH_a^o (kJmol-1)	ΔS_a^o (kJmol-1)
Blank	597.88	256.81	-33.51
200	917.91	576.83	-43.08

3.5. Potentiodynamic polarization

The corrosion of carbon steel in Chloride ion environment is an electrochemical corrosion comprises a simultaneous anodic dissolution of carbon steel and cathodic reduction reaction. To understand this mechanism of corrosion, the potentiodynamic polarization curves of carbon steel immersed in the absence and in presence of biotin at 30°C were obtained and shown in Figure 6. The potentiodynamic polarization curves of VB7 show both anodic and cathodic half-reactions of the carbon steel corrosion in 240 ppm Chloride ion environment. The change in the anodic and cathodic half-reaction curves was observed by the introduction of various concentrations of VB7 in the 240 ppm Chloride ion corrosion medium. The extrapolation of linear Tafel segments in these Tafel curves of VB7, the electrochemical corrosion parameters such as corrosion potential (E_{corr}), corrosion current (I_{corr}), cathodic slope (β_c), anodic slope (β_a), surface coverage area (θ) and percentage of inhibition efficiency were calculated from Tafel plots and were summarized in Table 1.

Table 5. Potentiodynamic polarization(PDP) parameter for carbon steel immersed in 240 ppm of aqueous chloride medium in the absence and presence of VB7.

Inhibitor concentration (PPM)	Blank I_{corr} (μAcm^{-2})	Inhibitor I_{corr} (μAcm^{-2})	E_{corr} (mV)/SCE	β_a (mV dec^{-1})	β_c (mV dec^{-1})	Surface coverage (θ)	IE_{PDP} (%)	IE_{WL} (%)
Blank	23.871	-	-316.816	162.689	128.447	0	-	-
VB7								
25	23.871	10.473	-199.832	126.594	76.74	0.56126	56.12	57.87
50	23.871	7.579	-265.324	86.468	93.031	0.68250	68.25	63.91
100	23.871	4.179	-182.549	69.199	97.653	0.82493	82.49	71.60
150	23.871	3.424	-223.089	98.629	72.365	0.85656	85.66	82.75
200	23.871	2.103	-182.478	87.453	77.082	0.91190	91.19	91.38

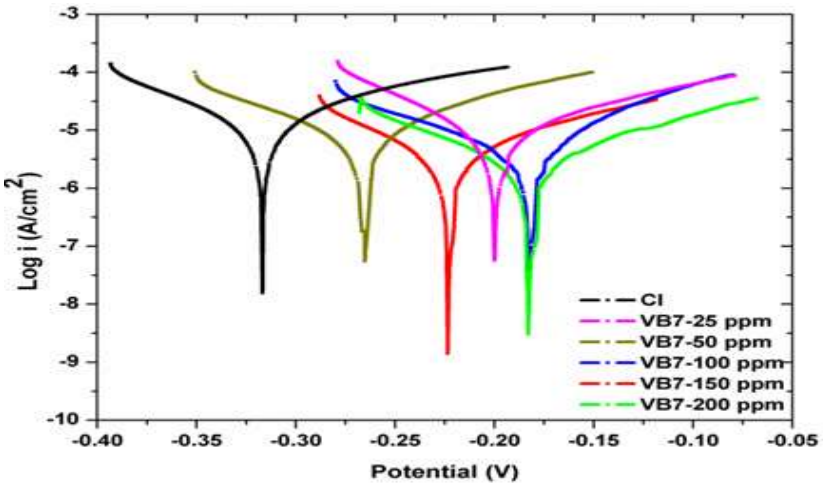

Figure 6. Potentiodynamic polarization curves for mild steel in 240 ppm aqueous chloride medium in the absence and presence of VB7.

The percentage of inhibition efficiency was then calculated using the equation[33]

$$\mathbf{IE\% = \left(\frac{I°corr - Icorr}{I°corr}\right) \times 100}$$

where $I°_{corr}$ and I_{corr} are the corrosion current density values in the absence and presence of VB7 respectively.

On increasing the concentration of VB7 from 25 to 200 ppm in the Chloride ion medium, the corrosion current density was reduced significantly (see Figure 2 and Table 1) and corrosion current density reached the minimum value for 200 ppm of VB7. The I_{corr} value decreases from 23.871 $\mu A/cm^{-2}$ for blank and reached the minimum value of 2.103 $\mu A/cm^{-2}$ for 200 ppm of VB7. This suggests that both anodic dissolution of carbon steel and cathodic reduction reaction were inhibited by the inhibitor VB7. The presence of inhibitor was blocking the active sites and modifying the carbon steel surface. This leads to the shift of anodic and cathodic slope areas toward lower current densities (I_{corr}). The percentage of inhibition efficiency (IE %) values obtained from the potentiodynamic polarization studies increased with increase in the concentration of the VB7 added to the corrosion medium. This implies that the corrosion inhibition of carbon steel was due to the formation of the adsorption film of VB7 formed on the surface of the carbon steel. The IE% values obtained from polarization studies also agreed well with the values of weight loss measurements.

The type of behavior of inhibitors VB7 was determined by relating the corrosion potential (E_{corr}) values. Generally, if the value of E_{corr} is greater than 85 mV/SCE the inhibitor can be classified as cathodic or anodic type and in addition, if the value of E_{corr} is lower than 85 mV/SCE the inhibitor can be classified as mixed-type.[34,35]The trend in the values of E_{corr} for VB7 showed a change greater than 85 mV/SCE and was within

the range (-316.816 mv/SCE to -182.478 mV/SCE) of 134.338 mV/SCE for VB7. This type of behavior of VB7 was attributed to either cathodic or anodic type inhibitor. But, the trend in the E_{corr} values of VB7 was not consistent with the increase or decrease in E_{corr} values from the blank value which suggested that VB7 was a mixed-type indicator in 240 ppm Chloride ion corrosion medium. However, the cathodic current densities were less sensitive and in the anodic range, a significant increase in the anodic current densities compared to cathodic current densities for various concentration of VB7 leads to the shift of the E_{corr} toward anodic direction. These observations confirmed that addition of VB7 in 240 ppm Chloride ion corrosion medium will reduce anodic dissolution of carbon steel more than the cathodic reduction reaction. This shows that the VB7 inhibits the corrosion mechanism by controlling anodic reaction predominantly which indicates that the VB7 was acted as anodic inhibitor in 240 ppm Chloride ion corrosion medium.

3.6. Electrochemical impedance spectroscopy

Electrochemical impedance spectroscopy is used to find out the kinetics and surface properties of the carbon steel corrosion in 240 ppm Chloride ion corrosion medium in the absence and in presence of VB7. Figure 7represents the Nyquist plots of carbon steel in 240 ppm Chloride ion corrosion medium in the absence and presence of VB7 at 30°C. Nyquist plots provide the value of charge transfer resistance (R_{ct}) and double layer capacitance (C_{dl}) andit is shown in the Table 6. Simple electrical equivalent circuit [36-37] is used to explain the nature of impedance, the resistor (R_s), resistance of charge transfer (R_{ct}) and a double layer capacitance (C_{dl}). The equivalent electrical circuit used to fit the impedance spectra was shown in Figure. 8.

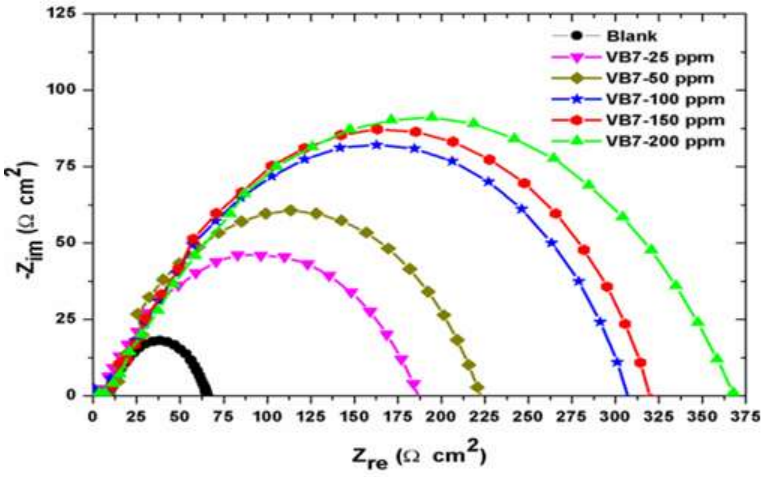

Figure 7. Nyquist plots for mild steel in 240 ppm aqueous chloride medium in the absence and presence of VB7.

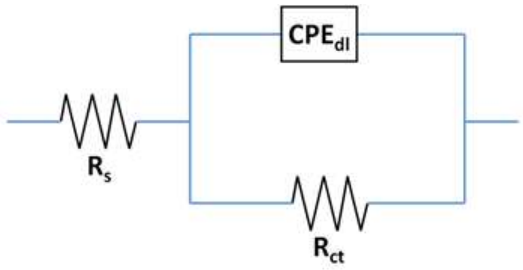

Figure 8. Equivalent electrical circuit used to fit the impedance spectra obtained for mild steel in 240 ppm aqueous chloride medium in the absence and presence of VB7.

CPE_{dl} is the constant phase equivalent of double layer, R_{ct} is the charge transfer resistance, and R_s is the solution resistance shown in the equivalent electrical circuit. Nyquist plots shows that when the concentration of VB7 increases the diameter of the semicircles (R_{ct}) increases which indicate the formation of protective film on the surface of carbon steel. As a result of increase in concentration of VB7, charge transfer resistance (R_{ct}) increased and decreased the double layer capacitance (C_{dl}) values. This was due to the adsorption of VB7 on the metal surface leading to the formation of a protective layer on the carbon steel surface and decreased the extent

of dissolution reaction which prevented the further corrosion of carbon steel.[38]The observed C_{dl} decreases due to decrease in dielectric constant because of increase in the thickness of the electrical double layer by the adsorption of inhibitors on carbon steel. The IE (%) was calculated from R_{ct} values through the following equation

$$\mathbf{IE\%} = \left(\frac{R_{ct(i)} - R_{ct(b)}}{R_{ct(i)}} \times \mathbf{100}\right)$$

where $\boldsymbol{R_{ct(b)}}$ and $\boldsymbol{R_{ct(i)}}$ were uninhibited and inhibited charge transfer resistance, respectively. The values of IE (%) were summarized in the Table 6.

Table 6.Potentiodynamic polarization parameter for carbon steelimmersed in 240 ppm of aqueous chloride medium in the absence and presence of VB7.

Inhibitor concentration (ppm)	R_{ct}(blank) (Ω cm^2)	$R_{ct(i)}$ (Ω cm^2)	Y_{max}	C_{dl} (μ F cm^{-2})	IE (%)	$\theta_{(imp)}$
VB7						
25	62.316	197	98.5	8.21E-06	68.36	0.6836
50	62.316	252.43	126.215	5E-06	75.31	0.7531
100	62.316	318.79	159.395	3.13E-06	80.45	0.8045
150	62.316	362.19	181.095	2.43E-06	82.79	0.8279
200	62.316	465.37	232.685	1.47E-06	86.60	0.8660

3.7 Analysis of adsorbed film

The scraped samples collected from coupons immersed in 240 ppm Chloride ion medium was labeled as "MS in Cl" and scraped samples collected from coupons immersed in the same chloride medium with VB7 were labeled as "MS in VB7+Cl", and were used in the below discussion.

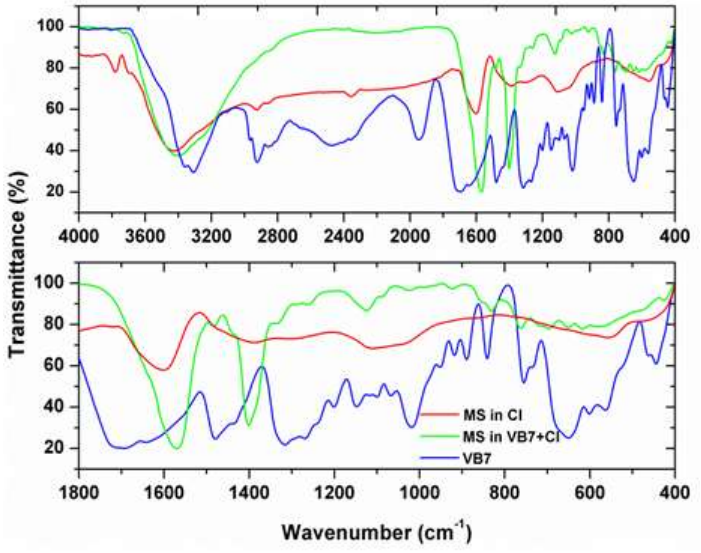

Figure 9.FTIR spectra of MS in chloride medium, MS in VB7 and chloride medium and VB7.

FTIR spectra in Figure 9 were recorded for MS in Cl, MS in VB7+Cl and VB7 samples. The strong bands at 1708 cm^{-1} and 1240 cm^{-1} were assigned to the ureido carbonyl stretching and cyclic urea stretching of fused rings of VB7.[39-40] The strong peaks at 1571 cm^{-1} and 1408 cm^{-1} were due to the carboxylate group of VB7 in completely ionized form.[41] The disappearance of 1708 cm^{-1} and 1240 cm^{-1}peak implied that there was an interaction of ureido ring with the carbon steel surface and appearance of strong peaks at 1571 cm^{-1} and 1408 cm^{-1} indicated that the carboxylic group in VB7 exists in ionized form in the 240 ppm Chloride ion medium.

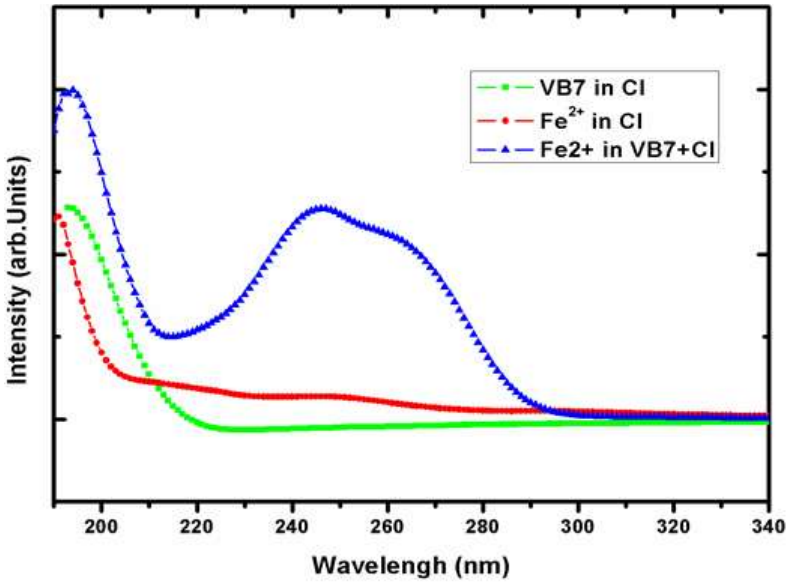

Figure 10.UV-Vis spectra for VB7 system in 240 ppm chloride ion medium.

The UV-Vis absorption spectroscopy is a suitable method for identification of complex ions in solution and with the change in position of the absorption maximum indicates the formation of a complex between two species in solution. The UV-Vis absorption spectrum in Figure 10 was taken for 240 ppm Chloride ion medium containing 200 ppm of VB7 and 300 ppm of Fe ($FeSO_4$). The absorption spectrum for VB7 in Chloride ion medium had absorption maximum at only 193 nm. After 24 h, the absorption curve for VB7+ Fe in Chloride ion medium exhibited small shift in absorption band, which indicated the complex formation between VB7 and Fe.

3.8. Surface analysis

Scanning Electron Microscopy (SEM) images and their corresponding Energy Dispersive Spectroscopy (EDX) spectra were obtained and shown in Figure 11 and Figure 12. The smooth surface was the carbon steel surface before immersion (see Figure. 11(a)). After immersion in 240 ppm Chloride ion medium, the roughness due to pits was observed in the carbon steel surface shown in Figure 11(b). Figure 11(c) represents the images of carbon steel immersed in VB7.

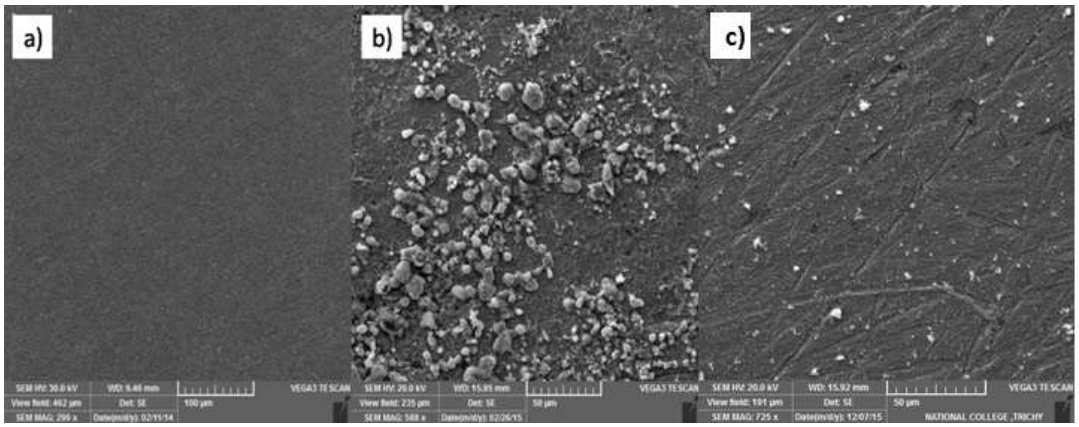

Figure 11. SEM images of surface of mild steel: a) polished mild steel, b) mild steel immersed in 240 ppm of aqueous chloride medium and mild steel immersed in 240 ppm of aqueous chloride medium in presence of c) VB7.

On comparing the SEM images, it was evident that the VB7 was adsorbed on the surface of the carbon steel which was indicated by the smooth surface in the Figure 11(c). In Figure 11(c), the patches were due to accumulated VB7 on the adsorbed carbon steel surface. The corresponding EDX spectra to the SEM image

Figures 11(a) to 11(c) were shown in Figures 12(a) to 12(c). In Figure 12(b), the presence of Chloride ion was responsible for the pitting in the carbon steel seen in Figure 11(b). Sodium ions were confirmed to have no influence on the corrosion behavior.[42] The absence of Chloride ion in Figure 12(c) implied that the inhibitor VB7 was adsorbed on the carbon steel which was indicated by the presence of nitrogen and sulphur in EDX spectra (see Figure 12(c)) and smooth SEM images of VB7 (see Figure 11(c)). The protective adsorbed film of VB7 prevented the contact of Chloride ion to the metal surface and prevented the further corrosion of carbon steel.

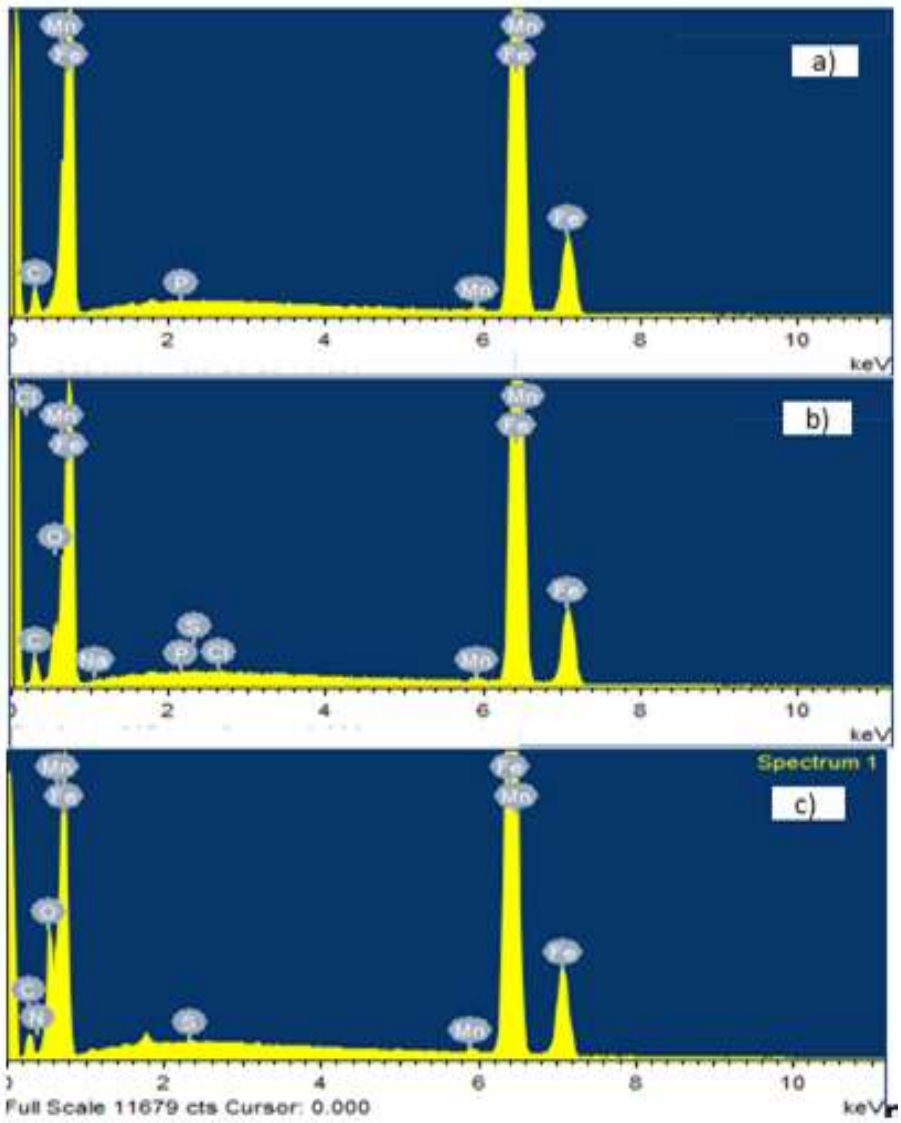

Figure 12.EDX spectra of the surface of mild steel: a) polished carbon steelb) carbon steel immersed in 240 ppm of aqueous chloride medium and c) carbon steel immersed in 240 ppm of aqueous chloride medium in presence of VB7.

3.9. Quantum chemical calculation

This theoretical approach helps to find the corrosion inhibition effectiveness which depends on the molecular structure. The calculated quantum chemical parameters related to the inhibition effect of VB7 such as the energy of the highest occupied molecular orbital (E_{HOMO}), the energy of the lowest unoccupied molecular orbital (E_{LUMO}), the gap energy ΔE_{gap}, the dipole moment (μ), the electronegativity (χ), the global hardness (γ), the global softness (σ) and the total energy (E_T) were calculated and listed in Table 7. The Optimized geometries for (a) VB7 and Electrostatic potential surface of compound (b) VB7, distribution of HOMO energy of (c) VB7 and distribution of LUMO energy of (d) VB7 were shown in Figure 13.

Table 7.Quantum chemical parameters for VB7 calculated by DFT/B3LYP method.

Vitamin	E_{HOMO} (eV)	E_{LUMO} (eV)	ΔE_{gap} (eV)	μ (Debye)	x	Γ	σ	Total Energy (a.u)
VB7	-6.250	0.305	6.555	2.999	3.277	2.972	0.336	-1124.10

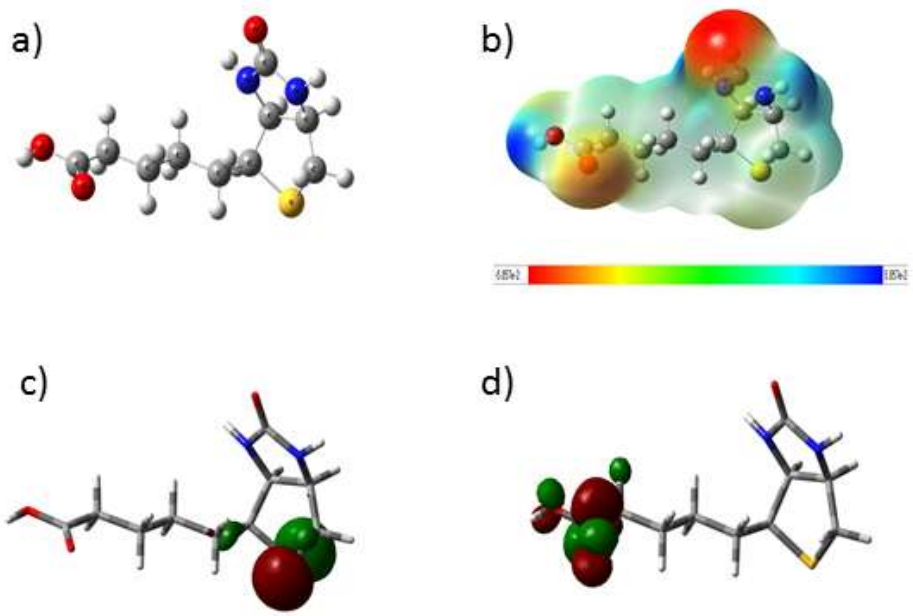

Figure 13.Optimized geometries for (a) VB7 and Electrostatic potential surface of compound (b) VB7, distribution of HOMO energy of (c) VB7 and distribution of LUMO energy of (d) VB7.

A molecule to be effective corrosion inhibitor, it must donate electrons to the vacant d orbital of the metal for bonding and/or receive free electrons from the metal surface.[43] The frontier molecular orbital are involved in the bonding between the corrosion inhibitor and the metal surface. The frontier molecular orbital are highest occupied molecular orbital (HOMO) and lowest unoccupied molecular orbital (LUMO). The difference in energies i.e. energy gap ($\Delta E=E_{LUMO} - E_{HOMO}$) of the HOMO and the LUMO of the corrosion inhibitor is considered for the effective chemical adsorption of the inhibitor (reactivity) on the metal surface. Higher energy of the HOMO (E_{HOMO}) indicates the electron donating ability of the inhibitor molecule to the unoccupied d-orbital of the metal and lower energy of the LUMO (E_{LUMO}) indicates the electron accepting ability of the inhibitor molecule from the metal. Larger the ΔE value implies that the inhibition efficiency of the inhibitor is less due to low reactivity with the metal surface and lower the ΔE value implies that the inhibitor is having higher inhibition efficiency due to high reactivity with metal surface. [43-46]

The dipole moment (μ) and electronegativity (x) are important quantum chemical parameter which represents the distribution of electrons in the molecular structure and electron attracting capacity of the molecule, respectively. High value of μ probably increases the inhibitor adsorption through electronic force.[47] The dipole moments of VB7 are 2.999 Debye, which indicates that there are strong dipole–dipole interactions between VB7 and metal surface. In addition to that, VB7 possess high electronegativity x_{VB7}(3.277) and so VB7 gets adsorbed on the metal surface strongly and has high inhibition efficiency. Global hardness (γ) and global softness (σ) are another important property to measure the reactivity of an inhibitor.

4. Conclusion

1. The vitamin VB7 act as worthy corrosion inhibitors for carbon steel in 240 ppm Chloride ionsolution. Their inhibition efficiencies increase with increasing concentration of inhibitors. The values of the

inhibition efficiency of 200 ppm VB7 acquired from the weight loss measurement at 240 ppm Chloride ion solution were 91.37%.

2. The inhibition efficiency of VB7 increased with optimum pH, and decreased with temperature.
3. The adsorption of VB7 obeys the Langmuir adsorption isotherm. The adsorption process is a spontaneous and endothermic process accompanied by a decrease of entropy.
4. The vitamin VB7 act as mixed–type inhibitors without changing the mechanism of hydrogen evolution that is confirmed by potentiodynamic polarization studies.
5. The electrochemical impedance studies of VB7 in 240 ppm Chloride ion solution confirmed that the charge transfer resistance increases, whereas the double layer capacitance reduces. This is due to the thickness of electrical double layer formed by the adsorption of VB7 on the surface of carbon steel.
6. The formation of Fe−VB7 complex was undoubtedly indicated by UV−visible spectrophotometric studies and adsorption of VB7 on the carbon steel surface was confirmed by FT-IR spectra.
7. The adsorption of VB7 on the carbon steel was also confirmed by the presence of nitrogen and sulphur signal in EDX spectra.
8. The difference in surface morphology of carbon steel surface due to formation of protective layer by VB7 was confirmed by SEM image.
9. From the DFT calculations, the frontier molecular orbitals such as HOMO and LUMO showed that the studied inhibitors adsorb through the active centers (O, S and N atoms) and ureido ring and carboxyl group of VB7.
10. The theoretical studies are in close agreement with the experimental results; it showed that VB7 are good organic inhibitors.

References:

1. Szklarska-Smialowska, Z. and J. Mankowski, *Crevice corrosion of stainless steels in sodium chloride solution.* Corrosion Science, 1978. 18(11): p. 953-960.
2. Oldfield, J.W., *Test techniques for pitting and crevice corrosion resistance of stainless steels and nickel-base alloys in chloride-containing environments.* International Materials Reviews, 1987. 32(1): p. 153-172.
3. Frankel, G.S., *Pitting Corrosion of Metals: A Review of the Critical Factors.* Journal of The Electrochemical Society, 1998. 145(6): p. 2186-2198.
4. Niu, L.-B. and K. Nakada, *Effect of chloride and sulfate ions in simulated boiler water on pitting corrosion behavior of 13Cr steel.* Corrosion Science, 2015. 96(0): p. 171-177.
5. Sanyal, B., *Organic compounds as corrosion inhibitors in different environments — A review.* Progress in Organic Coatings, 1981. 9(2): p. 165-236.
6. Raja, P.B. and M.G. Sethuraman, *Natural products as corrosion inhibitor for metals in corrosive media — A review.* Materials Letters, 2008. 62(1): p. 113-116.
7. Gece, G., *Drugs: A review of promising novel corrosion inhibitors.* Corrosion Science, 2011. 53(12): p. 3873-3898.
8. Bouklah, M., et al., *Thiophene derivatives as effective inhibitors for the corrosion of steel in 0.5 M H2SO4.* Progress in Organic Coatings, 2004. 49(3): p. 225-228.
9. Yohai, L., M. Vázquez, and M.B. Valcarce, *Phosphate ions as corrosion inhibitors for reinforcement steel in chloride-rich environments.* Electrochimica Acta, 2013. 102: p. 88-96.
10. Kosari, A., et al., *Electrochemical and quantum chemical assessment of two organic compounds from pyridine derivatives as corrosion inhibitors for carbon steel in HCl solution under stagnant condition and hydrodynamic flow.* Corrosion Science, 2014. 78: p. 138-150.
11. Yadav, M., et al., *New pyrimidine derivatives as efficient organic inhibitors on carbon steel corrosion in acidic medium: Electrochemical, SEM, EDX, AFM and DFT studies.* Journal of Molecular Liquids, 2015. 211: p. 135-145.
12. Al-Sarawy, A.A., A.S. Fouda, and W.A.S. El-Dein, *Some thiazole derivatives as corrosion inhibitors for carbon steel in acidic medium.* Desalination, 2008. 229(1–3): p. 279-293.
13. Hejazi, S., et al., *Electrochemical and quantum chemical study of Thiazolo-pyrimidine derivatives as corrosion inhibitors on carbon steel in 1 M H2SO4.* Journal of Industrial and Engineering Chemistry, 2015. 25: p. 112-121.

14. Bereket, G., E. Hür, and C. Öğretir, *Quantum chemical studies on some imidazole derivatives as corrosion inhibitors for iron in acidic medium.* Journal of Molecular Structure: THEOCHEM, 2002. 578(1–3): p. 79-88.
15. Fang, J. and J. Li, *Quantum chemistry study on the relationship between molecular structure and corrosion inhibition efficiency of amides.* Journal of Molecular Structure: THEOCHEM, 2002. 593(1–3): p. 179-185.
16. Yıldız, R., et al., *Experimental studies of 2-pyridinecarbonitrile as corrosion inhibitor for carbon steel in hydrochloric acid solution.* Corrosion Science, 2014. 82: p. 125-132.
17. Morad, M.S.S., A.E.-H.A. Hermas, and M.S.A. Aal, *Effect of amino acids containing sulfur on the corrosion of carbon steel in phosphoric acid solutions polluted with Cl−, F− and Fe3+ ions–behaviour near and at the corrosion potential.* Journal of Chemical Technology & Biotechnology, 2002. 77(4): p. 486-494.
18. Chirkunov, A. and Y. Kuznetsov, *Chapter 4 - Corrosion Inhibitors in Cooling Water Systems*, in *Mineral Scales and Deposits*, Z.A.D. Demadis, Editor. 2015, Elsevier: Amsterdam. p. 85-105.
19. Patni, N., S. Agarwal, and P. Shah, *Greener Approach towards Corrosion Inhibition.* Chinese Journal of Engineering, 2013. 2013: p. 10.
20. Sekine, I., Y. Nakahata, and H. Tanabe, *The corrosion inhibition of carbon steel by ascorbic and folic acids.* Corrosion Science, 1988. 28(10): p. 987-1001.
21. Malhotra, S. and G. Singh, *Vitamins: potential inhibitors for nickel in acidic media.* Surface Engineering, 2005. 21(3): p. 187-192.
22. Solmaz, R., *Investigation of corrosion inhibition mechanism and stability of Vitamin B1 on carbon steel in 0.5 M HCl solution.* Corrosion Science, 2014. 81: p. 75-84.
23. Fuchs-Godec, R. and G. Zerjav, *Corrosion resistance of high-level-hydrophobic layers in combination with Vitamin E – (α-tocopherol) as green inhibitor.* Corrosion Science, 2015. 97(0): p. 7-16.
24. Abiola, O.K., et al., *3-[(4-amino-2- methyl-5-pyrimidinyl) methyl]-5- (2-hydroxyethyl)-4-methyl thiazolium chloride hydrochloride as green corrosion inhibitor of copper in HNO3 solution and its adsorption characteristics.* Green Chemistry Letters and Reviews, 2011. 4(3): p. 273-279.
25. Tomic, R.F.G.M.G.P.M.V., *The Inhibitive Effect of Vitamin-C on the Corrosive Performance of Steel in HCl Solutions.* International Journal of Electrochemical Science, 2013. 8(1): p. 1511-1519.
26. Hoseizadeh Ali, R., I. Danaee, and H. Maddahy Mohammed, *Thermodynamic and Adsorption Behaviour of Vitamin B1 as a Corrosion Inhibitor for AISI 4130 Steel Alloy in HCl Solution*, in *Zeitschrift für Physikalische Chemie International journal of research in physical chemistry and chemical physics*. 2013. p. 403.
27. W.A. Badawy, K.M. Ismail, A.M. Fathi, Electrochim.Corrosion control of Cu–Ni alloys in neutral chloride solutions by amino acids. Acta 51, 4182 (2006)
28. M.A. Migahed, H.M. Mohammed, A.M. Al-Sabagh,Corrosion inhibition of H-11 type carbon steel in 1 M hydrochloric acid solution by N-propyl amino lauryl amide and its ethoxylated derivatives. Mater. Chem. Phys. 80, 169 (2003)
29. A. Azim, L.A. Shalaby, H. Abbas,Mechanism of the corrosion inhibition of Zn Anode in NaOH by gelatine and some inorganic anions. Corros. Sci. 14, 21 (1974)
30. M. Hosseini, S.F.L. Mertens, M.R. Arshadi, Synergism and antagonism in mild steel corrosion inhibition by sodium dodecylbenzenesulphonate and hexamethylenetetramine. Corros. Sci. 45, 1473 (2003)
31. S.T. Arab, K.M. Emran,Thermodynamic study on Corrosion Inhibition of Fe78B13Si9 Metallic Glass Alloy in Na2SO4 Solution at Different Temperatures Int. J. Appl. Chem. 3, 69 (2007)
32. X.H. Li, G.N. Mu, Inhibition effect of tetradecylpyridinium bromide on the corrosion of cold rolled steel in 7.0 M H3PO4 Appl. Surf. Sci. 252, 1254 (2005)
33. Ashassi-Sorkhabi, H., Z. Ghasemi, and D. Seifzadeh, *The inhibition effect of some amino acids towards the corrosion of aluminum in 1 M HCl + 1 M H2SO4 solution.* Applied Surface Science, 2005. 249(1–4): p. 408-418.
34. Singh, A.K. and M.A. Quraishi, *Investigation of adsorption of isoniazid derivatives at carbon steel/hydrochloric acid interface: Electrochemical and weight loss methods.* Materials Chemistry and Physics, 2010. 123(2–3): p. 666-677.
35. Verma, C., M.A. Quraishi, and A. Singh, *5-Substituted 1H-tetrazoles as effective corrosion inhibitors for carbon steel in 1 M hydrochloric acid.* Journal of Taibah University for Science, 2016. 10(5): p. 718-733.

36. RIBEIRO, D.V., C.A.C. SOUZA, and J.C.C. ABRANTES, *Use of Electrochemical Impedance Spectroscopy (EIS) to monitoring the corrosion of reinforced concrete.* Revista IBRACON de Estruturas e Materiais, 2015. 8: p. 529-546.
37. Mansfeld, F., *Electrochemical impedance spectroscopy (EIS) as a new tool for investigating methods of corrosion protection.* Electrochimica Acta, 1990. 35(10): p. 1533-1544.
38. Umoren, S.A., et al., *Inhibition of carbon steel corrosion in H2SO4 solution by coconut coir dust extract obtained from different solvent systems and synergistic effect of iodide ions: Ethanol and acetone extracts.* Journal of Environmental Chemical Engineering, 2014. 2(2): p. 1048-1060.
39. Socrates, G., ed. *Infrared and Raman Characteristic Group Frequencies*. 3rd ed. 2001, John Wiley & Sons Ltd: West Sussex, England.
40. Lapin, N.A. and Y.J. Chabal, *Infrared Characterization of Biotinylated Silicon Oxide Surfaces, Surface Stability, and Specific Attachment of Streptavidin.* The Journal of Physical Chemistry B, 2009. 113(25): p. 8776-8783.
41. Barbucci, R., et al., *Antigen–antibody recognition by Fourier transform IR spectroscopy/attenuated total reflection studies: Biotin–avidin complex as an example.* Biopolymers, 1991. 31(7): p. 827-834.
42. Hirano, M., et al., *Accelerated Corrosion Behavior due to Alternating Dry-Wet Conditions for LP Steam Turbine Materials of Fossil Power Plants.* ISIJ International, 2005. 45(3): p. 373-379.
43. Gece, G., *The use of quantum chemical methods in corrosion inhibitor studies.* Corrosion Science, 2008. 50(11): p. 2981-2992.
44. Khalil, N., *Quantum chemical approach of corrosion inhibition.* Electrochimica Acta, 2003. 48(18): p. 2635-2640.
45. Masoud, M.S., et al., *The role of structural chemistry in the inhibitive performance of some aminopyrimidines on the corrosion of steel.* Corrosion Science, 2010. 52(7): p. 2387-2396.
46. Ghailane, T., et al., *Experimental and theoretical studies for carbon steel corrosion inhibition in 1 M HCl by two new benzothiazine derivatives.* Corrosion Science, 2013. 76: p. 317-324.
47. Zhang, F., et al., *Performance and theoretical study on corrosion inhibition of 2-(4-pyridyl)-benzimidazole for carbon steel in hydrochloric acid.* Corrosion Science, 2012. 61: p. 1-9.

*****